July 1987
LU TP 87-10

Parton Showers in Leptoproduction Events

Mats Bengtsson, Torbjörn Sjöstrand
Department of Theoretical Physics,
University of Lund, Sölvegatan 14A,
S-223 62 Lund, Sweden

Abstract:

We present a model that includes the production of arbitrarily many jets in lepton-hadron events, using the leading log formalism for parton shower evolution. The main problem encountered here, which has not previously been illuminated by studies of e^+e^- annihilation or Drell-Yan/$Z^0/W^\pm$ production, is the choice of kinematics in the spacelike shower evolution. In our preferred solution, the standard definition of Bjorken x is preserved during the construction of initial and final state showers - a nontrivial constraint. The resulting model is described in detail, including some first investigations of its properties.

1. Introduction

As machines are designed for higher and higher energies, QCD bremsstrahlung phenomena become more and more important. SPS has so far provided lepton-hadron events at an invariant mass of 23 GeV - enough to observe sizable bremsstrahlung corrections to the event shape [1] -, while TeV II gives roughly 35 GeV. HERA will come into operation in a couple of years and will then provide data at an invariant mass of 315 GeV. Machines at even higher energies, like LEP + LHC, are under discussion.

The two alternatives that exist to calculate parton final states are matrix elements and, using the Altarelli-Parisi equations, parton showers. Matrix element calculations are exact, order by order in α_s, but technical complications limit the calculations to the first few orders. The advantage with parton showers is that the whole series expansion in α_s is included, admittedly in an approximate fashion, the leading log approximation.

Phenomenological models based on $O(\alpha_s)$ matrix elements have been shown to describe SPS data fairly well [1,2], while no comparisons with parton showers have yet been made. In e^+e^- physics at 30 GeV it has been shown [3] that not even second order matrix elements [4] are sufficient to describe the data accurately. First order matrix elements are obviously faring even worse, leaving us with a parton shower picture which is superior to $O(\alpha_s^2)$ calculations even at these fairly low energies. A similar phenomenon could therefore be expected in leptoproduction at high energies.

One aspect should always be kept in mind, however: the level of accuracy in fragmentation studies is less in leptoproduction than in e^+e^-. On the theoretical side, because of the nonperturbative initial state, the hadron, which introduces a number of uncertainties: structure functions, initial state showers (structure function evolution), hadron remnants, etc. On the experimental side because particles are measured in a laboratory frame which is generally boosted with respect to the hadronic CM frame, because interactions occur in the t-channel so that small scattering angles dominate, because hadron remnants usually disappear down the beam pipe, etc.

With the advent of HERA and higher energies, it becomes important to explore the parton shower alternative. We will here present a first attempt to construct a model, with particular emphasis on uncertainties in the theoretical assumptions. There are basically two ingredients that go into our model for leptoproduction, final state showers and initial state showers. Final state or timelike parton showers are by now well studied in e^+e^- physics [3,5,6]. There are a number of investigations made from different sets of data, which all show a very good agreement between models and data. Initial state or spacelike showers in hadron-hadron collisions are revealed e.g. in the p_T spectrum of $W^\pm$ and Z^0. This has also been studied [7,8], but the constraints on the model from data are here weak.

The outline of this paper is as follows. In the next section a detailed description of the different components in the model is presented. Particular emphasis is put on problems specific to leptoproduction. In section 3 follows basic studies of the model, with emphasis on parton level results. A brief summary is given in section 4. Comparisons with experimental data and with the matrix element approach are postponed to a second paper, which also will contain predictions for higher energies.

2. The Model

2.1. General Overview

The kinematical variables used in leptoproduction are assumed well known, but are briefly reviewed for the sake of completeness. Consider an interaction in the naive parton model, Fig. 1. The following relations then hold:

$$\begin{aligned} q &= k - k' \ , \\ Q^2 &= -q^2 = -(k-k')^2 \ , \\ x &= \frac{Q^2}{2Pq} \ , \\ y &= \frac{Pq}{Pk} \ , \\ W^2 &= (P+q)^2 = \frac{1-x}{x} Q^2 + m_p^2 \ . \end{aligned} \tag{1}$$

It is also common to define ν, the boson energy in the rest frame of the hadron, and s, the total invariant energy squared.

The basic structure of the cross-section, before any QCD radiation is taken into account, may generically be written as

$$d\sigma = (\text{boson propagator}) \times (\text{parton distributions}) \times \\ \times (\text{lepton-boson-parton couplings}) \times (\text{helicity factors}). \tag{2}$$

One distinguishes between neutral current (NC) events, with γ/Z exchange, and charged currents (CC) ones, with $W^{\pm}$ exchange. The full structure of the NC, including interference terms between γ and Z^0, is rather complicated. The dominant contribution comes from the term with simple γ exchange

$$\frac{d\sigma}{dxdy} = \frac{4\pi\alpha_{em}^2}{sx^2y^2}\left(1 - y + \frac{y^2}{2}\right) \sum_i e_i^2 \, xf_i(x,Q^2) \tag{3}$$

where the index i enumerates the quark and antiquark flavours, e_i is the corresponding electric charge, and $f_i(x,Q^2)$ is the usual hadron structure function. In our calculations the full propagator, including Z^0 and interference terms, is taken into account. No effects of initial state polarizations or initial state photon radiation [9] are included, however. Neglected is also the contribution from longitudinally polarized photons, which is of the order of 10% at present energies, and is expected to decrease with energy.

The first order corrections ($O(\alpha_s)$) to the simple parton model picture were calculated a couple of years ago [10,11], and have been implemented in Monte Carlo programs [2,12]. A complete $O(\alpha_s)$ calculation includes virtual corrections to the parton model results above, but in particular it includes two completely new final states, Fig. 2. In the first one, a gluon is emitted from either initial or final quark leg, while the second one, the photon-gluon fusion diagram, contains a quark-antiquark pair in the final state.

In a discussion of parton showers, it is necessary to distinguish between initial state showers, where the branches occur before the photon vertex, and final state showers, where they occur after the photon vertex, Fig. 3. The separation of these two possible time orderings implies a neglect of the interference terms in Fig. 2, and is of course not gauge invariant. In the collinear regions, close to the incoming or outgoing parton directions, the correct results should still be obtained, while wide angle emission could be misrepresented. In e^+e^- physics this problem was possible to overcome, at least partially, by matching on to the lowest order matrix elements. Here it is considerably more difficult to perform the corresponding analysis.

If one may view a complete interaction at the hadronic side in a "chronological" order, the initial state consists of a set of partons, close to mass-shell ($\approx$ 1 GeV), whereof one initiates a cascade. In each branch of this cascade, one of the daughters continues towards the hard interaction vertex with increasing spacelike virtuality, while the other one is on mass-shell or acquires a timelike virtuality (in which case it will develop a timelike shower of its own). The spacelike shower is therefore characterized by increasing Q^2, decreasing energies and increasing (average) opening angles. Once the incoming spacelike quark has been struck by the boson, the outgoing quark is now timelike, or at least on mass-shell. This timelike quark starts to shower into daughters with decreasing masses. In the shower, the opening angles between daughters are decreasing, as are the daughter energies. The basic behaviour of initial and final state showers alike is regulated by the Altarelli-Parisi equations [13], but with important differences as to details, as will be discussed later on.

In matrix element calculations all external legs are on mass-shell and, because of the inclusion of interference terms, it is not meaningful to ask what is the virtuality of intermediate partons. The situation is quite the opposite in parton shower algorithms, where the generation of spacelike or timelike masses is a central ingredient. This leads to complications in the definition of the Bjorken x variable, as follows, Fig. 3. From the kinematics of the lepton vertex, the Bjorken x is unambiguously defined as $x = Q^2/2Pq$. It is also possible to define an $x' = p_1q/Pq$, i.e. (in the Breit frame, i.e. in the frame where the boson four-vector is $q = (0; 0, 0, Q)$) the longitudinal momentum of the struck quark as a fraction of the momentum of the original proton. These two coincide for massless incoming and outgoing partons, since then

$$0 = p_1'^2 = (p_1 + q)^2 = p_1^2 + 2p_1q + q^2 = x'2Pq - Q^2 \\ \rightarrow \quad x' = \frac{Q^2}{2Pq} = x. \tag{4}$$

If the incoming parton has a spacelike virtuality $p_1^2 = -Q_1^2$ and/or the outgoing parton a timelike virtuality $p_1'^2 = m_1'^2$, this relation is changed to

$$m_1'^2 = p_1'^2 = (p_1 + q)^2 = p_1^2 + 2p_1q + q^2 = -Q_1^2 + x'2Pq - Q^2 \\ \rightarrow \quad x' = \frac{Q^2 + Q_1^2 + m_1'^2}{2Pq} = x\left(1 + \frac{Q_1^2 + m_1'^2}{Q^2}\right). \tag{5}$$

Serious mismatches may thus occur between x and x'; in extreme cases even with

$x' > 1$. Although kinematically possible, such situations would cause other problems in the model. A possible solution will be presented in the next section.

The usual interpretation of the structure function $f_i(x,Q^2)$ is that it gives the probability to find a parton with flavour i, taking a fraction x of the hadron energy or momentum, if the hadron is probed at the "scale" Q^2 (i.e. with a boson spacelike virtuality Q^2). The exact choice of energy and momentum combination in the x definition is obviously irrelevant for massless partons (and negligible transverse momenta), but matters if partons are off mass-shell. Experimentally, structure functions are determined by measurements of the scattered lepton. In order to reproduce the correct differential cross-section, eq. (3), one is therefore obliged to use the Bjorken x definition, i.e. let the lepton vertex be unaffected by the evolution of parton showers. The alternative would have been to find a completely new set of structure functions, e.g. in terms of the x' defined above, based on an explicit model for the distribution of parton virtualities - a major task.

2.2. Spacelike Showers

The partons inside a hadron may be viewed as undergoing a continuous process of branchings and recombinations. Each branching a→bc involves some relative transverse momentum between the partons b and c. In a language where four-momentum is conserved at each vertex, this implies that at least one of the b and c partons must have a spacelike virtuality. Since the partons are virtual, a cascade only lives a finite time before reassembling, with the most off-shell partons living the shortest time. In a hard scattering, the larger the momentum transfer scale is (which for simplicity is taken equal to Q^2), the smaller are the distances probed in the hadron, and the softer is the parton composition observed. This is expressed by the Altarelli-Parisi evolution equations [13]

$$\frac{df_b(x,t)}{dt} = \frac{\alpha_s(t)}{2\pi} \sum_a \int \frac{dx'}{x'} f_a(x',t)\, P_{a\to bc}\left(\frac{x}{x'}\right). \tag{6}$$

Here the $f_i(x,t)$ are the usual structure functions and t is shorthand for $\ln(Q^2/\Lambda^2)$. Thus the first order strong coupling constant is

$$\alpha_s(Q^2) = \frac{12\pi}{(33-2n_f)t} = \alpha_s(t) \tag{7}$$

where n_f is the number of flavours. Finally, the Altarelli-Parisi splitting kernels $P_{a\to bc}(z)$ are given by

$$\begin{aligned} P_{q\to qg}(z) &= \frac{4}{3}\,\frac{1+z^2}{1-z}, \\ P_{g\to gg}(z) &= 6\,\frac{(1-z(1-z))^2}{z(1-z)}, \\ P_{g\to q\bar{q}}(z) &= \frac{1}{2}\,(z^2+(1-z)^2). \end{aligned} \tag{8}$$

The presence of a hard interaction reduces a cascade to a single sequence of branchings a→bc, where a and b are on the main chain of increasing spacelike virtuality, while $m_c^2 \geq 0$. A "forwards" evolution scheme, where the evolution of the shower is traced from some initial Q_0^2 up to the hard scale Q^2, is awkward technically, since it is then difficult to match up the spacelike shower with the hard interaction cross-section, and since the kinematics can not be constructed until it is known which branch is the one struck by the virtual photon. Instead a "backwards" evolution scheme has been developed [8], where the spacelike parton shower is reconstructed from the hard interaction backwards, i.e. in falling Q^2 sequence. This method is reviewed briefly in the following three paragraphs.

The Altarelli-Parisi equations express that, during a small increase dt there is a probability for a parton a with momentum fraction x' to become resolved into a parton b at $x = zx'$ and a parton c at $x'-x = (1-z)x'$. Correspondingly, during a decrease dt a parton b may be "unresolved" into a parton a. The conditional probability dP_b for this to happen is given by df_b/f_b which, using eq. (6), becomes

$$dP_b = \frac{df_b(x,t)}{f_b(x,t)} = |dt|\,\frac{\alpha_s(t)}{2\pi} \sum_a \frac{dx'}{x'}\,\frac{f_a(x',t)}{f_b(x,t)}\, P_{a\to bc}\left(\frac{x}{x'}\right) \tag{9}$$

Summing up the cumulative effect of many small changes dt, the probability for no radiation exponentiates. Therefore one may define a "Sudakov" form factor

$$S_b(x,t_{max},t) = \exp\left\{-\int_t^{t_{max}} dt'\,\frac{\alpha_s(t')}{2\pi} \sum_a \int dz\, P_{a\to bc}(z)\,\frac{x' f_a(x',t')}{x\, f_b(x,t')}\right\} \tag{10}$$

giving the probability that a parton b remains at x from t_{max} to $t < t_{max}$.

A knowledge of S_b is enough to trace the evolution backwards. The virtuality (the t value) of parton b is essentially obtained directly from eq. (10); a number of technical complications are described in [8]. For a given t of a branching, the relative probabilities for different allowed branchings $a \to bc$ are given by the z integrals in the sum in eq. (10). Finally, with t and a known, the probability distribution in the splitting variable $z = x/x' = x_b/x_a$ is given by the z integrand in eq. (10). With parton b given, the process may now be repeated for parton a to find its virtuality and origin, and so on until a virtuality is chosen below some small cutoff scale Q_0^2, which typically is taken to be 1 GeV^2.

In order to explicitly construct the four-momenta of the partons in the showers, and in particular the transverse momenta at branchings, a precise z definition is required. In the limit where virtualities are small compared to energies, and where transverse momenta are also small, all definitions of z should only differ by terms of order Q^2/s. Differences occur in general, however, and a given definition may be chosen for technical simplicity. In hadron-hadron collisions the preferred choice is the "$\hat{s}$ approach", where one requires that $\hat{s} = x_1 x_2 s$, both at the hard scattering and at any lower scale, i.e. $\hat{s}(Q^2) = x_1(Q^2)x_2(Q^2)s$, with $x_1(Q^2)$ and $x_2(Q^2)$ the x values at a given stage in the shower. In leptoproduction physics, the only change would be to replace one of the incoming partons by a nonradiating lepton at $x_2 = 1$. As an example, referring to Fig. 3, the z value of the branching $3 \to 1 + 2$ is given by $z = (p_1+k)^2/(p_3+k)^2$. With this definition made, and a random azimuthal angle chosen, the kinematics at the vertex is almost completely fixed. What remains to be specified is the mass of the associated timelike leg c, to be determined by the evolution of a timelike shower.

The $\hat{s}$ approach is very convenient e.g. when studying the production properties of W/Z bosons at hadron colliders, since the W/Z mass is preserved during the reconstruction of the initial state showers. The resulting model gives good agreement with the experimental W/Z p_T spectrum and other properties [8]. Unfortunately, in leptoproduction in this scheme the Bjorken x of the event is not preserved during the reconstruction of the initial state shower, since the introduction of transverse momenta at the branchings will shift the value of the product Pq. (This is most easily seen in the frame where the lepton and the hard scattering quark come in along the $\pm z$ axis. The backwards reconstruction of a shower is then completely symmetric with respect to an overall azimuthal rotation, i.e. the ϕ value of the shower initiating proton may be chosen arbitrarily. The product Pq, on the other hand, explicitly

depends on the relative azimuthal angle between the proton and the virtual photon.) The problem is illustrated in Fig. 4, where the finally reconstructed x distribution is shown for events with fixed original x and y values. This mismatch does not necessarily mean that the $\hat{s}$ scheme is wrong but only that the original cross-section, eq. (3), is changed by this method of handling the spacelike cascade. By a reweighting procedure it would be possible to overcome this drawback but, as noted before, this is a major task.

It is therefore desirable to find a scheme in which the x and Q^2 values of the event are unaffected by the parton shower properties. This is possible if the shower evolution does not refer to lepton momenta, except in the combination $q = k-k'$. It is not possible, however, to use the $\hat{s}$ approach with k just replaced by q: the $\hat{s}$ of the photon-quark hard scattering is $\hat{s} = (p_1+q)^2 = p_1'^2$, which might very well be vanishing. Instead a different approach is adopted. For this, consider the branching $3 \to 1 + 2$, Fig. 3. Since the z_1 to be defined for this branching should be Lorentz invariant, the allowed combinations of q, p_1 and p_3 may be parametrized as

$$z_1 = \frac{2p_1q + \alpha Q^2 + \beta Q_1^2}{2p_3q + \alpha Q^2 + \beta Q_3^2} \tag{11}$$

where α and β give the subleading contributions. The most straightforward choice would have been to put $\alpha = \beta = 0$ in eq. (11). Unfortunately, this means that z values are not bounded from above by unity. To see this, consider a collinear branching $3 \to 1 + 2$ in the Breit frame, where $z_1 = p_{1z}/p_{3z}$. If $Q_3^2 = 0$ and $Q_1^2 > 0$, then $|p_{1z}| > |p_{3z}|$ is perfectly allowed, since it is possible to have the recoiling parton 2 moving in the opposite direction; indeed this is required kinematically for $m_2^2 = 0$.

While the choice $\beta = 0$ has to be rejected, it is still desirable to put $\alpha = 0$: for a collinear branching with $Q_1^2 = Q_3^2 = m_2^2 = 0$ and $p_3 = P$, z_1 then coincides with the Bjorken x definition, i.e. the naive parton model is reproduced. A study shows that the requirement of z values bounded by unity is most easily fulfilled for $\beta = -2$, i.e.

$$z_1 = \frac{p_1q - Q_1^2}{p_3q - Q_3^2} = \frac{p_1(p_1+q)}{p_3(p_3+q)}. \tag{12}$$

The kinematics of branchings can now be constructed by analogy with the formulae in [8], as follows. First assume that q and p_1 are along the $\pm z$ axis, with q given by its hadronic CM frame form $q = (W^2-Q^2;\ 0,\ 0,\ W^2+Q^2)/2W = (q_0;\ 0,\ 0,\ q_z)$. In terms of the combinations

$$\begin{aligned} s_1 &= (p_1 + q)^2 + Q^2 + Q_1^2, \\ s_3 &= \frac{s_1 - 2Q_1^2}{z_1} + 2Q_3^2, \\ r_1 &= \{s_1^2 - 4Q^2Q_1^2\}^{1/2}, \\ r_3 &= \{s_3^2 - 4Q^2Q_3^2\}^{1/2}, \end{aligned} \tag{13}$$

the maximum virtuality of the timelike parton 2 in the branching $3 \to 1 + 2$ is given by

$$(m_2^2)_{max} = \frac{s_1 s_3 - r_1 r_3}{2Q^2} - Q_1^2 - Q_3^2. \tag{14}$$

With the maximum virtuality given, a timelike parton shower algorithm may be used to give the development of the subsequent cascade, including the actual mass m_2^2, with $0 \leq m_2^2 \leq (m_2^2)_{max}$.

Using the further relation $m_2^2 = p_2^2 = (p_3-p_1)^2$, the momentum of parton 3 (in this frame) may now be found as

$$\begin{aligned} E_3 &= \frac{1}{2}\,\frac{p_{1z}s_3 + q_z(Q_1^2+Q_3^2+m_2^2)}{p_{1z}q_0 - E_1 q_z}, \\ p_{3z} &= \frac{1}{2}\,\frac{E_1 s_3 + q_0(Q_1^2+Q_3^2+m_2^2)}{p_{1z}q_0 - E_1 q_z}, \\ p_{T3}^2 &= E_3^2 - p_{3z}^2 + Q_3^2 = \{(m_2^2)_{max} - m_2^2\}\,\frac{(s_1 s_3 + r_1 r_3) - 2Q^2(Q_1^2+Q_3^2+m_2^2)}{2r_1^2}. \end{aligned} \tag{15}$$

This completes the construction of the $3 \to 1 + 2$ vertex. The $q + p_3$ subsystem may now be boosted and rotated to bring p_3 along the $-z$ axis, while leaving q unchanged. When the next vertex is considered, $5 \to 3 + 4$ in Fig. 3, the $q + p_3$ system fills the function the $q + p_1$ did above. Once the shower initiator has been constructed and oriented, this fixes the frame in which also the incoming proton is along the $-z$ direction.

For each branching $a \to bc$, x_a and x_b must be used in the evaluation of structure functions. Up to this point, it has been assumed implicitly that the Bjorken x should be used for the parton closest to the hard interaction, $x_1 = x$, with preceding ones obtained from the z values constructed in the shower: $x_3 = x_1/z_1$, $x_5 = x_3/z_3$, etc. These x_j values should, in some sense, represent the ratio of four-momenta between partons p_j and the initial hadron. While this ratio is ambiguous for virtual partons, it is straightforward to define for the on-shell cascade initiator. In Fig. 5 is plotted the ratio $p_{z,init}/(x_{init}P_z)$, which clearly shows a severe mismatch between $x_{init}P_z$ and $p_{z,init}$. This mismatch is built up from a number of "subleading" contributions, and ought to disappear when all virtualities become small. The following expression is easily calculable

$$\begin{aligned} \frac{p_{init}q}{Pq} &= \frac{x}{\Pi z_j}\left(1 + \frac{m_1'^2 + Q_1^2}{Q^2}\right)\left(1 - \frac{2Q_1^2}{Q^2 + Q_1^2 + m_1'^2}\right) = \\ &= \frac{x}{\Pi z_j}\left(1 + \frac{m_1'^2 - Q_1^2}{Q^2}\right). \end{aligned} \tag{16}$$

Thus there are evidently two sources for the mismatch. The first factor comes from the difference between $(p_1q)/(Pq)$ and the Bjorken x, as discussed earlier, eq. (5). The other factor originates from the subleading parts (nonzero α and/or β) in the definition of z. As it turns out, the first factor dominates over the last, and one may experience a situation where $x_{init} < 1$ but $p_{z,init} > P_z$. This is clearly a pathological situation which must be cured.

The most straightforward solution, which is also the one adopted, is to redefine the first x used in the evolution according to

$$x_1' = x_1\left(1 + \frac{m_1'^2 - Q_1^2}{Q^2}\right). \tag{17}$$

This gives exact agreement between $p_{z,init}$ and $x_{init}P_z$, Fig. 5. It should be emphasized that the x redefinition is only used for the internal dynamics of the cascade, and can be thought of as a natural consequence of the choice of kinematics. The place where it does matter is in the ratio of structure functions in the "Sudakov form factor", eq. (10). The proper solution there would be a new tailormade set of structure functions, i.e. the problem we tried to avoid comes back to haunt us. Here it does not affect the differential cross-section $d\sigma/dxdy$, however, but only the amount of parton shower evolution. Since effects anyhow should tend to cancel partly in the

ratio of structure functions, the problem will be neglected.

A final note. In the section above, Q^2 has been used to denote a particle virtuality or an argument in α_s and in structure functions. It is in the nature of perturbative QCD that the definition of Q^2 in α_s is not unique. In particular, loop calculations tend to indicate that the proper argument for α_s is not Q^2 but $p_T^2 \approx (1-z)Q^2$ [14]. Such corrections can be taken into account if desired.

2.3. Timelike Showers

The timelike or final state showers appear for the quark scattered off the current q and, less importantly, for the side branches of the initial state cascade. The following discussion will be concentrated on the former case, with the latter obtained by a fairly straightforward generalization, given eq. (14). In order to describe the timelike shower evolution, the model presented in [6] will be used. This model is developed for e^+e^- annihilation events, where there are two cascading partons, which may balance energy and momentum internally when the partons are given masses. In leptoproduction, with only one final state parton to be evolved, special problems will arise, similar to those experienced with the spacelike cascade.

One possibility is to follow the route used in the case of hadron physics, i.e. let the two hard scattered particles radiate as a system. For leptoproduction this means the scattered lepton, k', and the scattered quark, p_1'. Here the scattered lepton does not radiate but, if the scattered parton acquires a mass, the momentum k' of the lepton has to be changed in the process, i.e. neither Q^2 nor Bjorken x is preserved. The shift in x is illustrated in Fig. 6, for events generated with initial values x = y = 0.2. As in the spacelike case, this scheme is not wrong per se, but merely inconvenient.

Instead we will follow another route, which is to evolve the scattered parton in the hadronic CM frame, without any reference to incoming or outgoing lepton momenta. More specifically, for the first branching 1' → 2' + 3', a splitting variable z_1' is defined by

$$z_1' = \frac{p_0 p_2'}{p_0 p_1'}, \tag{18}$$

where $p_0 = P + q$. In the hadronic rest frame $p_0 = (W; 0, 0, 0)$, and z_1' reduces to $z_1' = E_2'/E_1'$, i.e. energy fractions. The p_0 is kept as "reference vector" in subsequent branchings, i.e., for 2' → 4' + 5', $z_2' = (p_0 p_4')/(p_0 p_2') = E_4'/E_2'$, etc. Some other alternatives exist as options [6], but are not discussed here. Because of the choice of frame, the maximum kinematically allowed mass of the shower is $(m_1')_{max} = E_1' = W/2$. In section 3.1, the question of dynamically allowed masses will be discussed further.

If x = 0.5, the energy in the hadronic CM frame of the incoming quark (p_1) and of the scattered one (p_1') coincide. In the limit where the respective virtual masses are small, the phase space for emitting a soft or collinear gluon (z close to unity) is equal for the spacelike and timelike showers, given the z definitions we have adopted, eq. (12) and eq. (18). In this sense the two cascade schemes are consistent.

With the choice of z variable made, the evolution of a parton in the cascade is once again given by a Sudakov form factor, which expresses the probability that a parton a does not branch between some initial maximum mass-square m^2 and a minimum value m_0^2

$$S_a(m^2) = \exp\left\{-\int_{m_0^2}^{m^2} \frac{dm'^2}{m'^2} \int_{z_-(m')}^{z_+(m')} dz\, \frac{\alpha_s(Q^2)}{2\pi} P_{a\to bc}(z)\right\}. \tag{19}$$

The Altarelli-Parisi kernels, $P_{a\to bc}(z)$, are identical with those given in eq. (8). The Sudakov form factor can be used to find the mass of the decaying parton, the z value in its branching and the flavours of the daughters. These daughters may be evolved in their turn, and so on. The shower is traced down to some minimum cutoff virtuality m_0^2 (here taken to be 1 GeV^2).

A number of special features of timelike showers are known and included. One is coherence among soft gluons, which leads to angular ordering: the opening angles of branches are constrained to decrease monotonically as the masses are evolved downwards [15]. Another aspect is the freedom to use different scales as argument in α_s, as in the spacelike case. Studies of coherence effects [16] suggest that the $p_T^2 \approx z(1-z)m^2$ of the daughters is preferrable to use as an argument. In order not to get unacceptably large values of α_s, a constraint $p_T^2 \approx z(1-z)m^2 \geq m_0^2/4$ must be imposed.

The evolution of spacelike and of timelike parton showers have been considered separately above. In order to complete the description of this scheme, the two components have to be put together, as follows. With x and Q^2 chosen from the cross-section, eq. (3), it is straightforward to construct q, p_1 and p_1', put along the z axis in the hadronic CM frame, with p_1 and p_1' on mass-shell. The timelike quark leg p_1' is evolved and acquires a mass m_1'. While the energy is preserved in the process, the longitudinal momentum is not. Before considering momentum conservation, the spacelike leg is evolved, to give $p_1^2 = -Q_1^2$, and the four-momentum p_1 is constructed such that $m_1'^2$ is taken into account in the equations in section 2.2. At the end of the spacelike cascade evolution, an on-mass-shell initiator parton is constructed, wiht momentum p_{init}. By virtue of the rotations and boosts performed in connection with each branching, p_{init} is along the z axis, as is the unchanged q vector, while p_1 now has a transverse momentum. The four-momentum $p_1' = p_1 + q$ of the timelike shower initiator is now known, and the timelike shower already constructed can be boosted and rotated to give agreement. After the hadron remnant has been added, the system can be boosted from the hadronic CM frame to any desired frame.

2.4. Other Issues

A number of other issues remain to be discussed before the description of the model may be considered complete. String fragmentation [17] has proven to be a very successful scheme, is thoroughly tested together with parton showers in e^+e^- physics [3,6], and will be used here throughout. A string is stretched from a colour triplet (quark, antidiquark), via a number of octets (gluons) to end at an antitriplet (antiquark, diquark). Several strings in one single event is perfectly allowed. In each branching of a parton shower, $q \to qg$, $g \to gg$ and $g \to q\bar{q}$, the colour flow is well defined, so that the way to connect the partons of an event with strings is unambiguous. This is not true for a general matrix element calculation, where non-planar Feynman diagrams sometimes give an undefined colour topology in the final state.

When dealing with the hadron remnant, three separate cases may be distinguished, depending on whether the spacelike shower initiator is a valence quark, a gluon or a sea quark. If the initator is a valence quark, the remnant is a diquark, which is just considered as an endpoint of a string. If the initiator is a gluon, then the three remaining valence quarks are in a

colour octet, with two strings attached. This state is conveniently subdivided into one diquark and one quark, and it must be specified how these should share the energy and momentum of the hadron remnant. With χ representing the E + p_L ($p_L = \pm p_z$, the longitudinal momentum) fraction taken by the quark, a form

$$P(\chi)d\chi = \frac{(1-\chi)^3}{(\chi^2 + c^2)^{1/2}}\, d\chi \tag{20}$$

is used [18]. Here, $c = 2m_q/s^{1/2} = 0.6$ GeV/$s^{1/2}$ gives a cut-off of the singularity at $\chi = 0$.

Similar energy sharing distributions are needed when a sea (anti)quark is emitted from the incoming hadron, producing a qqqq or $qqq\bar{q}$ colour triplet remnant. In these cases the remnant is split into a hadron plus a remainder jet: either a baryon plus a quark jet, or a meson plus a diquark jet. Flavours are combined taking into account that a sea $q\bar{q}$ pair comes from the splitting of a colour octet gluon so that, if one of the pair is kicked out, the other should end up in the hadron split off. Simple counting rules are here used for the energy sharing, based on the number of valence quarks in an object. Thus the χ fraction of the quark jet or the meson in the first or second case above, respectively, is given by

$$P(\chi)d\chi = 2(1-\chi)d\chi \quad . \tag{21}$$

The initiator parton may be assumed to have some primordial k_T, generated according to a Gaussian, typically with $\langle k_T^2 \rangle = (0.44\ \text{GeV})^2$. The recoil is then taken up by the hadron remnant. If the remnant is decomposed into two objects, these may be given a relative transverse momentum as well. The picture of a (massless) incoming hadron split into a parton shower initiator and a beam remnant, both massless and parallel to each other, is therefore slightly upset. The kinematical solution adopted is to consider the process as a longitudinal decay of the total invariant hadronic energy W into two subsystems with transverse mass-squares $(p_{init} + q)^2 + k_T^2$ and $p_{remnant}^2 + k_T^2$, respectively.

The machinery for target remnant treatment is, with minor modifications, taken over from PYTHIA version 4.8 [18], as is structure function parametrizations. For the results in this paper, we have used EHLQ set 1 [19], with $\Lambda = 0.2$ GeV. Fragmentation and timelike cascades are performed by JETSET version 6.3 [20].

3. Studies with the Model

With the whole machinery for generating parton and hadron configurations available in the form of a Monte Carlo program, there are a large number of interesting issues to be investigated. A first comparison of model and EMC data has been made, with good results, but the presentation of these investigations is postponed to a subsequent paper [21], where also extrapolations to HERA energies will be presented. The studies in this section are more intended to illuminate the properties of the model as such.

3.1. Studies on the Parton Level

In the probabilistic leading log picture, the spacelike and timelike showers factorize. In a complete quantum mechanical description, this separation is not gauge invariant, but for practical purposes one may accept it as a first approximation. That way it becomes possible to study the relative characteristics of the spacelike and the timelike cascades. In Fig. 7a is plotted the parton rapidity distributions in the hadronic CM frame, separately for the timelike and the spacelike showers. The two cascades are fairly well separated, i.e. to be found in the forward and in the backward hemisphere, respectively. The number of partons is obviously not an infrared safe quantity; a better representation is provided by the p_T-weighted rapidity distribution, Fig. 7b. The spacelike shower is here shown to be concentrated more towards the central rapidity region than the timelike one. This is simply because a large part of the hadron, the remnant, does not take part in the interaction, and ends up far out in the backwards hemisphere with negligible transverse momentum.

From Fig. 7b it is also obvious that the timelike shower generates more transverse momentum than does the spacelike one. Another measure of this difference is the average virtuality of outgoing and incoming parton at the boson vertex. Over essentially the whole region of x and y values, the average timelike mass $\langle m_1' \rangle$ is greater than the average spacelike mass $\langle Q_1 \rangle$ by a factor of two or three. As an example, Fig. 8a shows the timelike and spacelike mass distributions for HERA events with x = y = 0.2. Also if the hadron physics schemes are used for initial and final state showers (with limitations as discussed in sections 2.2 and 2.3, respectively), the same difference appears, see Fig. 8b, although the masses are slightly larger overall because of the larger phase space available when energy and momentum can be reshuffled. The

spacelike and timelike masses are neither gauge independent quantities nor experimentally observable ones. However, the consequence of the difference in masses is a larger jet activity in the forward than in the backward hemisphere, and this is indeed in agreement with matrix element results, both analytical [10] and Monte Carlo [2] ones, and with experimental observations at SPS energies [1]. This point will be returned to later.

In the language of parton showers, the asymmetry between spacelike and timelike masses may be understood as follows. The Sudakov form factors, eq. (10) and eq. (19), respectively, contains all the information for the choice of virtualities. Let us make a distinction between dynamics, which is essentially governed by the Altarelli-Parisi kernels and the structure functions, and kinematics, which is related to the amount of available phase space. The latter is conveniently gauged by $-\ln(1-z_{1+})$ where z_{1+} is the upper integration limit in the z integrals. For x reasonable large ($x \geq 0.3$) or large Q^2, the ratio of structure functions in eq. (10) is steeply falling with increasing x', i.e. decreasing z. This ratio, which is absent in the timelike case, is enough to give a large dynamical suppression. For smaller x, the ratio of structure functions is of the order of unity, and the dynamics in the two cases are fairly similar, but here the available phase space for emission is different. In the spacelike case $z_{1+} = 1 - Q_1^2/Q^2$, while in the timelike case $z_{1+}' \approx 1 - xm_1'^2/((1-x)Q^2)$, with the latter giving a larger phase space for small x.

One specific problem encountered in the parton shower approach is the question of maximum allowed virtuality, i.e. the question of scale. The scale could either be set by Q^2 or by W^2 or, more generally, by a combination of the two. Our experience from e^+e^- physics is no guide here, since $Q^2 = W^2$ in e^+e^- annihilation. A similar situation holds for initial state radiation in W/Z production, where the boson mass (or some multiple thereof) sets the only sensible scale. In leptoproduction, the standard statement is that Q^2 sets the scale for the resolution of partons, and therefore should govern the parton shower evolution. This is certainly not the full story, however. In the limit of $Q^2 \to 0$, i.e. photoproduction, such an argument would suggest the complete absence of perturbative QCD corrections, while in fact the process $\gamma + g \to q + \bar{q}$ is still allowed, here with a scale customarily related to the transverse mass of the produced quarks. It has also been noted that, with Q^2 as main scale for matrix element calculations in leptoproduction, the x dependent factors conspire to give a transverse energy flow mainly determined by W^2 for not too small x values [10,11].

In order to compare predictions of parton cascades, with different scales, and of matrix elements, it is convenient to choose a measure on the parton level which is infrared stable. A simple measure is the p_T sum of all partons in the hadronic CM frame. In Fig. 9 this spectrum is compared for the alternatives above. As expected, the spectrum is broader and reaches higher values of Σp_T in the W^2 case than in the Q^2 one. The W^2 shower alternative also has larger $\langle\Sigma p_T\rangle$ than the matrix elements; this is partly due to a difference in the hardest emission and partly due to the presence of extra soft partons in a shower approach. This plot was done for a certain set of cutoffs in x and y ($x \geqslant 0.01$, $y \geqslant 0.01$) and details do change somewhat if other values are chosen. Although no simple answer can be given, it is thus not unreasonable to use W^2 rather than Q^2 as a first approximation to the scale. Unless otherwise indicated, that is the choice in this paper.

As discussed above, there is a fairly strong asymmetry between parton emission in the forward and in the backward hemisphere. Another way to study this is to plot $dz/d\cos\theta$ in the hadronic rest frame, where z is some scaled energy variable. In the following, the symmetric definition $z_i = 2E_i/W$ has been used. This energy flow, weighted with the total cross-section, is plotted in Fig. 10 for a neutrino beam (CC) with $x = y = 0.2$, and HERA energy. Comparing matrix elements with parton showers, it is clear that the showers contribute with a large amount of extra radiation over the whole angular region, approximately a factor of two. The difference tends to be somewhat larger in the very backwards direction, where showers show more of a peaking than matrix elements.

3.2. Studies including Fragmentation

The addition of parton showers has several implications besides the previously discussed ones. The perhaps most direct test is in the charged multiplicity distribution, which should exhibit a stronger W dependence with showers than without, as follows. In the naive parton model, i.e. without showers, the multiplicity is expected to increase proportionally to lnW. When showers are included, essentially nothing is changed at low W, since the phase space here is too small for significant extra parton production anyway. With increasing energy more partons are being emitted in the showers, which leads to more complicated string configurations spanning the emitted partons (the string becomes "longer" than a straight one with the same W) and hence an extra

increase in multiplicity. Now, the string fragmentation scheme is infrared stable in the sense that, if a parton branches into two partons with a small invariant mass (either a soft or a collinear branching), the change on the particle level is minimal. Thus the increase in parton multiplicity is only partly mirrored in the particle multiplicity, i.e. the two are not proportional to each other. This is shown in Fig. 11 a and b, where the average parton multiplicity and the charged multiplicity are plotted as a function of lnW for SPS and HERA energies (23 GeV and 315 GeV invariant energy, respectively). Also shown is the scaling behaviour of the single string in the simple parton model, which is significantly below the shower model at typical HERA energies.

A further warning is in place. More partons in the final state does not necessarily mean more separately observable jets, since most partons are close to one another and are not resolvable in the particle final state. At HERA energies a number of well separated jets is predicted in some fraction of the events, and here parton showers offer a more detailed picture than is provided by the naive parton model or first order matrix elements. This will be discussed further in [21].

While the number of observable jets is not large, the current jet does become visibly broader by the sum total of emitted partons. The energy flow $dE/d\theta$ in HERA events is shown in Fig. 12, in the lepton scattering plane of the lab frame, for fix x and y values (0.2 and 0.5, respectively). While the beam jet receives only minor contributions from the cascade, the current jet becomes considerably wider, by approximately a factor of five. This significantly increases a slight difference in width between current and beam jet present already without showers. Energy flow in the regions between the jets is also increased by a factor of five in the case considered here.

As a final example, consider the average transverse momentum of charged particles, defined in the hadronic CM frame as a function of the Feynman x, Fig. 13. The strong asymmetry between forward and backward hemispheres already noted in section 3.2 is again visible. Notable is also that the characteristic seagull effect, i.e. a dip at $x_F = 0$, remains when the energy is increased from SPS to HERA (this dip has a kinematical origin and disappears if x_F is replaced by Y). The backward region is seen to receive rather small contributions from showers, while the forward region receives the major increase.

4. Summary

In this paper we have presented a detailed model for initial and final state parton showers in leptoproduction events. In view of our previous studies of final state radiation in e^+e^- annihilation [6] and initial state one in W/Z production [8], this might seem a straightforward task. Unfortunately, a subsidiary constraint is imposed by the desire to have the parton showers leave the x (and Q^2) value(s) of an event unchanged. This is trivial when partons are assumed massless and collinear, as in structure function evolution, but becomes more complicated when each parton branching is assumed to involve some transverse momentum and, as a consequence, the produced partons are not on mass-shell. It must be emphasized that the strive to preserve x is not required by theoretical consistency, but by experimental convenience: a standard task will be to predict event properties given that leptons are observed with momenta corresponding to some specific window of x and Q^2 values. The preservation of x also allows us to use already existing structure function parametrizations, which have been constructed to reproduce the differential cross-sections $d\sigma/dxdy$, rather than having to find ones of our own.

The problems noted above leads to a very specific choice for handling initial and final state cascades. When all is said and done, however, the resulting properties are very close to those obtained in a quite different scheme without explicit x preservation. There is one problem that does not receive an entirely satisfactory solution: that of the maximally allowed virtuality for parton shower evolution. Here one would like to match on to the known first order matrix elements. This was the approach in e^+e^- annihilation [6], but is much harder in leptoproduction, both because of the more complicated structure that needs to be described (including e.g. structure functions) and because an asymmetrical separation into maximum initial and final state virtualities is required. It seems that a reasonable overall agreement can be obtained with Q^2 as maximum allowed virtuality in the cascades; even in this case, however, a W dependence enters via the allowed phase space. if W^2 is significantly larger than Q^2, a parton shower evolution with maximum allowed virtuality Q^2 does not populate the full phase space accessed in the matrix element approach. Instead, with W^2 as scale, hard gluon emission may be overestimated, but this could then be corrected by ordinary Monte Carlo rejection techniques. Therefore the W^2 scale approach is the more promising one for an eventual matching on to first order matrix elements.

Another issue not covered here is coherence phenomena in initial state cascades (coherence in the final state showers is, however), which has recently been studied by Ciafaloni [22]. A Monte Carlo program incorporating coherence is in preparation by Marchesini and Webber [23], and should offer possibilities for interesting comparisons with our approach.

One nontrivial finding is that, with a sensible (but not gauge invariant) separation of initial and final state showers, the final state radiation dominates in magnitude by roughly a factor of three over essentially the whole range of x and Q^2 values. In hadron physics this difference is generally less, and in the small x region spacelike showers may there dominate over timelike ones.

In the short run, the model presented here can, and will [21], be used to compare with data at present energies. This will serve as a calibration point for the main application: to predict event shapes at HERA and other future high energy lepton-hadron colliders.

References

1. EMC Collaboration, J. J. Aubert et al., Phys. Lett. 95B (1980) 306, ibid. 100B (1981) 433
   EMC Collaboration, M. Arneodo et al., Phys. Lett. 149B (1984) 415

2. B. Andersson, G. Gustafson, G. Ingelman, T. Sjöstrand, Z. Physik C9 (1981) 233, ibid. C13 (1982) 361
   G. Ingelman, B. Andersson, G. Gustafson, T. Sjöstrand, Nucl. Phys. B206 (1982) 239

3. T. Sjöstrand, Z. Physik C26 (1984) 93
   JADE Collaboration, W. Bartel et al., Z. Physik C25 (1984) 231, ibid. C33 (1986) 23
   Mark II Collaboration, A. Petersen et al., Phys. Rev. Lett. 55 (1985) 1954, SLAC-PUB-4290/LBL-23243 (1987)
   S. Bethke, Heidelberg Habilitation thesis, LBL 50-208 (1987)
   T. Takahashi, Tokyo Ph.D. thesis, UT-HE-87/2 (1987)

4. A. Ali, J. G. Körner, Z. Kunszt, E. Pietarinen, G. Kramer, G. Schierholz, J. Willrodt, Nucl. Phys. B167 (1980) 454
   K. J. F. Gaemers, J. A. M. Vermaseren, Z. Physik C7 (1980) 81
   R. K. Ellis, D. A. Ross, A. E. Terrano, Nucl. Phys. B178 (1981) 421
   J. A. M. Vermaseren, K. J. F. Gaemers, S. J. Oldham, Nucl. Phys. B187 (1981) 301
   K. Fabricius, G. Kramer, G. Schierholz, I. Schmitt, Z. Physik C11 (1982) 315
   Z. Kunszt, Phys. Lett. 99B (1981) 429
   F. Gutbrod, G. Kramer, G. Schierholz, Z. Physik C21 (1984) 235
   T. D. Gottschalk, M. P. Shatz, Phys. Lett. 150B (1985) 451

5. G. Marchesini, B. R. Webber, Nucl. Phys. B238 (1984) 1
   B. R. Webber, Nucl. Phys. B238 (1984) 492

6. M. Bengtsson, T. Sjöstrand, Phys. Lett. 185B (1987) 435, Nucl. Phys. B289 (1987) 810

7. G. Altarelli, R. K. Ellis, M. Greco, G. Martinelli, Z. Physik C27 (1985) 617
   C. T. H. Davies, B. R. Webber, W. J. Stirling, Nucl. Phys. B256 (1985) 413

8. T. Sjöstrand, Phys. Lett. 157B (1985) 321
   M. Bengtsson, T. Sjöstrand, M. van Zijl, Z. Physik C32 (1986) 67

9. L. W. Mo, Y. S. Tsai, Rev. Mod. Phys. 41 (1969) 205
   S. Jadach, MPI-PAE/PTh 75/86 (1986)

10. G. Altarelli, G. Martinelli, Phys. Lett. 76B (1978) 89

11. R. Peccei, R. Rückl, Nucl. Phys. B162 (1980) 125

12. G. Ingelman, T. Sjöstrand, LU TP 80-12 (1980)
    G. Ingelman, LEPTO version 4.3, CERN program pool long writeup, program W5046 (1986)
    G. Ingelman, LEPTO version 5.1, private communication and in preparation

13. G. Altarelli, G. Parisi, Nucl. Phys. B126 (1977) 298

14. A. Bassetto, M. Ciafaloni, G. Marchesini, Phys. Rep. 100 (1983) 201

15. A. H. Mueller, Phys. Lett. 104B (1981) 161
    B. I. Ermolaev, V. S. Fadin, JETP Lett. 33 (1981) 269

16. D. Amati, A. Bassetto, M. Ciafaloni, G. Marchesini, G. Veneziano, Nucl. Phys. B173 (1980) 429
    G. Curci, W. Furmanski, R. Petronzio, Nucl. Phys. B175 (1980) 27

17. B. Andersson, G. Gustafson, G. Ingelman, T. Sjöstrand, Phys. Rep. 97 (1983) 33

18. H.-U. Bengtsson, T. Sjöstrand, LU TP 87-3/UCLA-87-001 (1987), to appear in Computer Phys. Comm.

19. E. Eichten, I. Hinchliffe, K. Lane, C. Quigg, Rev. Mod. Phys. 58 (1986) 1065

20. T. Sjöstrand, M. Bengtsson, Computer Phys. Comm. 43 (1987) 367
T. Sjöstrand, Computer Phys. Comm. 39 (1986) 347

21. M.Bengtsson, G. Ingelman, T. Sjöstrand, in preparation

22. M. Ciafaloni, CERN-TH.4672/87 (1987)

23. G. Marchesini, B. R. Webber, private communication

Figure Captions

Fig. 1. Kinematics notation for the simple case without any QCD corrections. Particles that appear "after" the boson vertex are always written with a prime. The proton four-momentum is denoted by capital P.

Fig. 2. The lowest order QCD corrections to the basic process in Fig. 1.

Fig. 3. Notations of a QCD process with initial and final state radiation included.

Fig. 4. Bjorken x divided by the input x used for generating events ($x = 0.2$, $y = 0.2$) in the $\hat{s}$ approach. Only initial state showers are switched on.

Fig. 5. The ratio $p_{z,init}/(x_{init}P_z)$ plotted for $x_1 = x_{Bj}$ in the initial state shower (dotted line), and for $x_1 = x_1'$ from eq. (17) (delta function at 1). Both x and y were fixed at 0.2.

Fig. 6. Bjorken x divided by the input x used for generating events ($x = 0.2$, $y = 0.2$) in the $\hat{s}$ approach. Only final state showers are switched on.

Fig. 7a. dn/dY on parton level in the hadronic CM frame, plotted separately for final state partons (dotted line), initial state partons (dash-dotted line) as well as the sum of the two (full line). The energy was fixed to 315 GeV and events were generated with cuts $x \geqslant 0.1$ and $y \geqslant 0.1$.

Fig. 7b. dp_T/dY with notation as in Fig. 7a.

Fig. 8a. Distribution of timelike mass m_1' (dotted line) and spacelike one Q_1 (full line), for $x = y = 0.2$ at HERA energy with standard kinematics.

Fig. 8b. As in Fig. 8a but now for the $\hat{s}$ approach.

Fig. 9. The distribution $dP/d\Sigma p_T$ at parton level in the hadronic CM frame, plotted for events at HERA energy with cuts $x \geqslant 0.01$, $y \geqslant 0.01$, $Q^2 \geqslant 4\ GeV^2$ and $W^2 \geqslant 2\ GeV^2$. Dash-dotted curve model results with Q^2 as scale, full with W^2 as scale and dashed for matrix elements [12]. The no-emission peaks at the origin are omitted; therefore the areas of the curves are slightly below unity.

Fig. 10. Energy flow for partons in the hadronic CM frame, $\sigma_{tot} dz/d\cos\theta$ as a function of $\cos\theta$ for $z = 2E/W$. Results are for a neutrino beam (CC) with $x = y = 0.2$, and where σ_{tot} is the total cross-section from the expression corresponding to eq. (3). The full line is for parton showers and the dash-dotted for matrix elements as implemented in the MC of [12].

Fig. 11. Multiplicity increase with W, a) for SPS energy, b) for HERA energy. The dotted line is the average charged multiplicity without any QCD corrections. The dash-dotted line is the average number of partons produced (the remnant is also counted in this case) and the full line is the average multiplicity for the parton shower model. Cuts as in Fig. 9.

Fig. 12. The energy flow in the event plane, $dE/d\theta$ plotted for configurations generated with fixed x (= 0.2) and y (= 0.5) at HERA energy. The full line is for the model, while the dashed one is without any QCD corrections. Direction of the scattered electron, scattered parton ("q") and target remnant ("qq") as given by the naive parton model.

Fig. 13. Predicted average p_T for charged particles plotted as a function of Feynman x ($x_F = 2p_z/W$) in the hadronic CM frame. Full line is for SPS energy and the dotted one for HERA energy. The cuts are identical with the ones in Fig. 9.

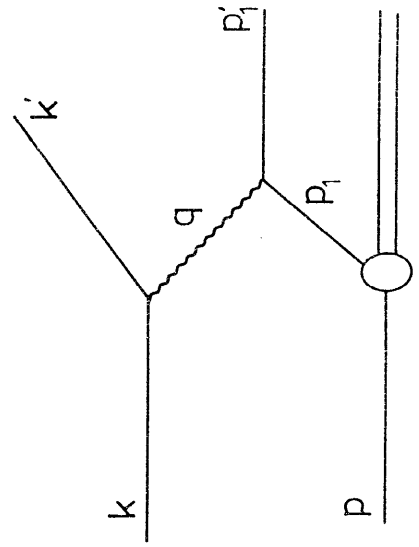

Fig. 1

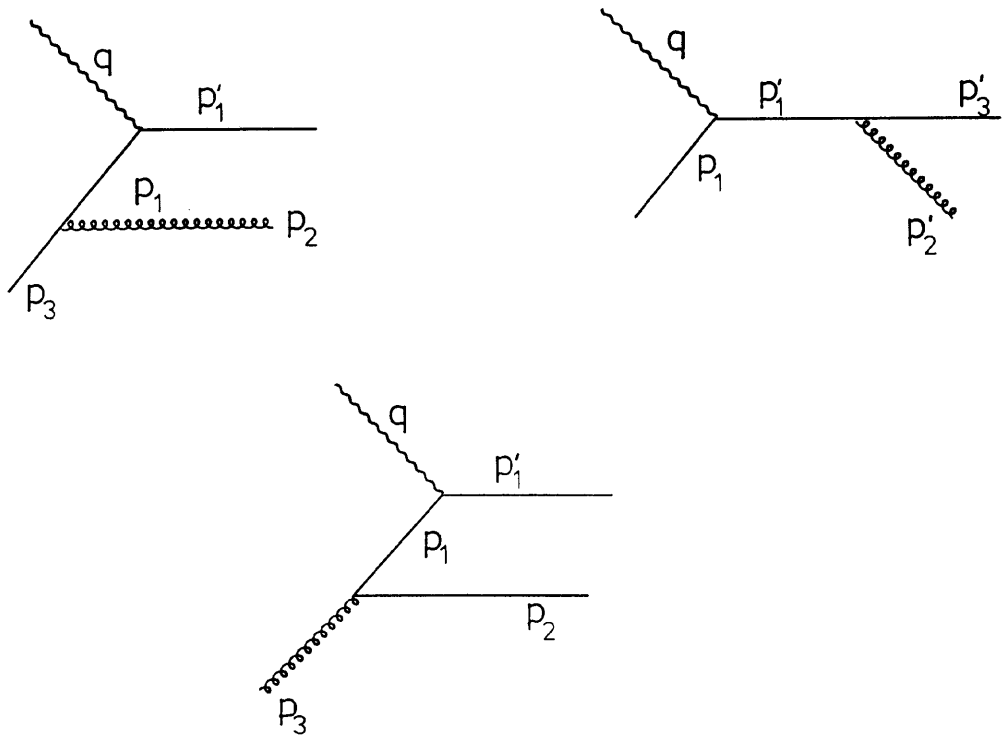
q
p'1
p1
p2
p3
q
p'1
p'3
p1
p'2
q
p'1
p1
p2
p3

Fig. 2

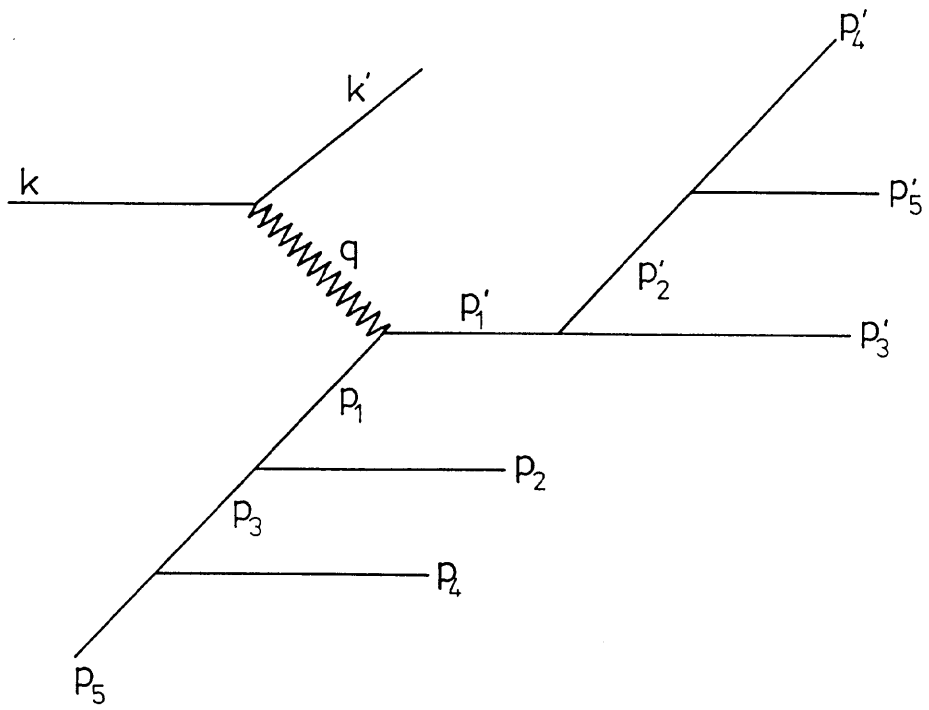
p'4
k'
k
p'5
q
p'2
p'1
p'3
p1
p2
p3
p4
p5

Fig. 3

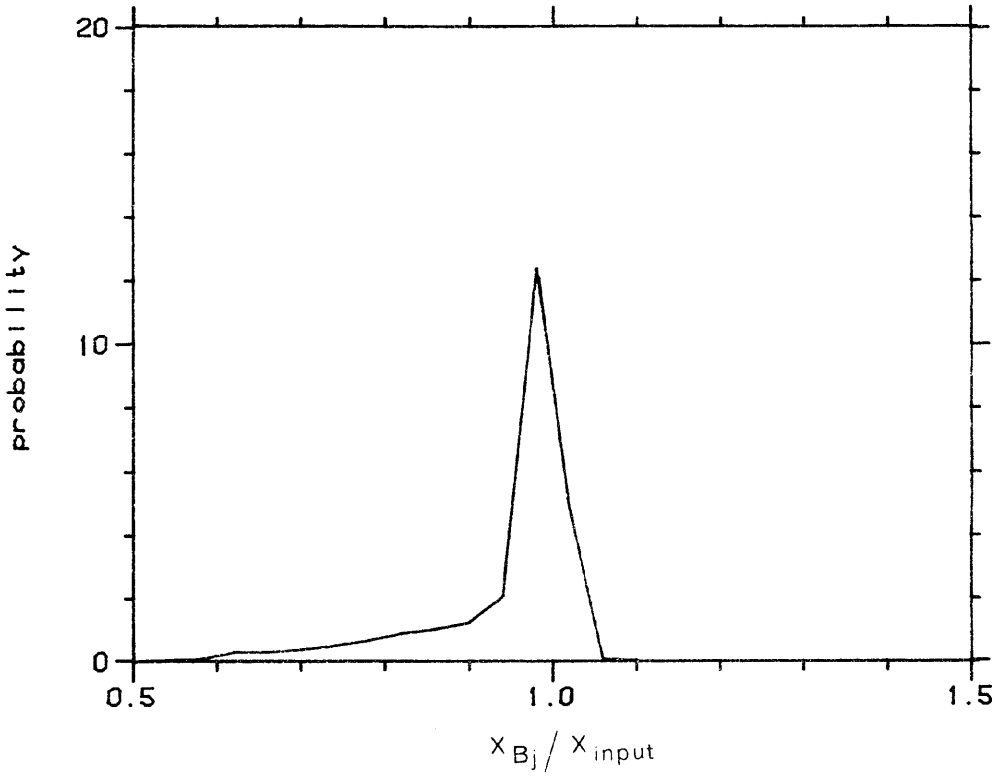
20
10
0
probability
0.5
1.0
1.5
x_{Bj} / x_{input}

Fig 4

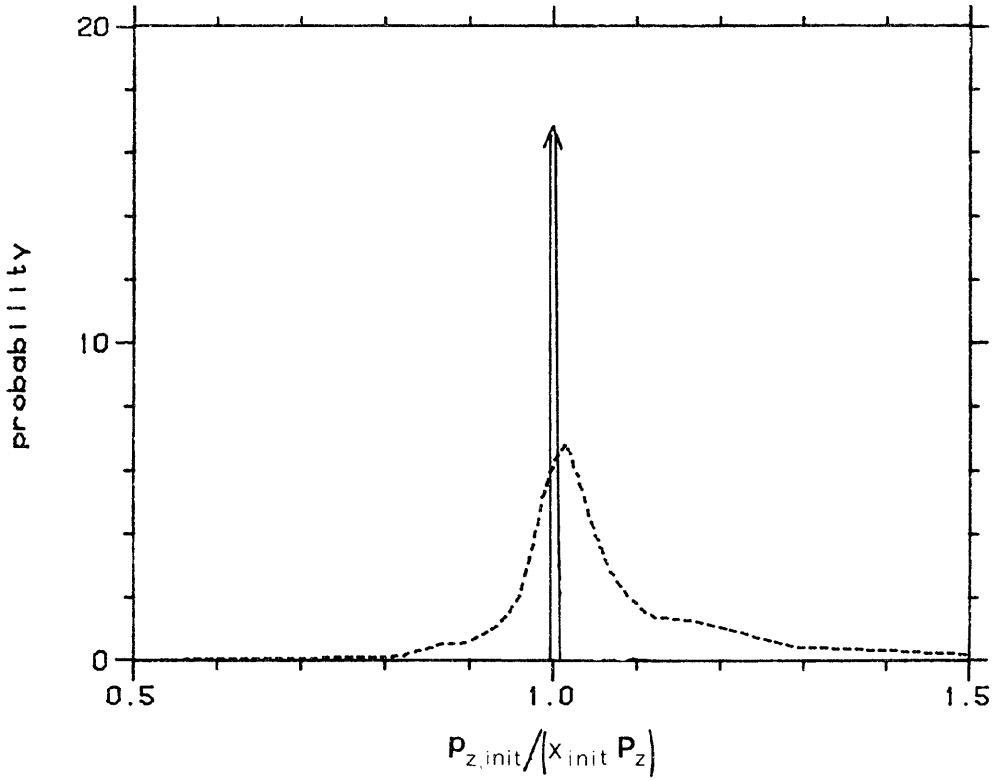
20
10
0
probability
0.5
1.0
1.5
$p_{z,init}/(x_{init}\, p_z)$

Fig 5

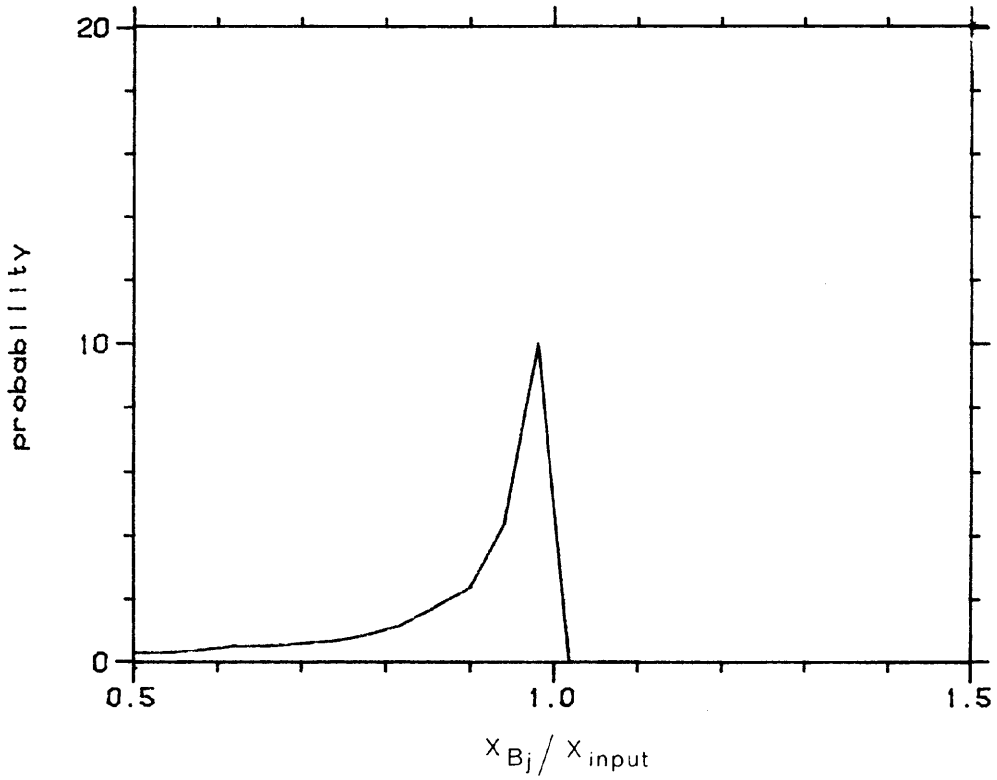
20
10
0
probability
0.5
1.0
1.5
x_{Bj} / x_{input}

Fig 6

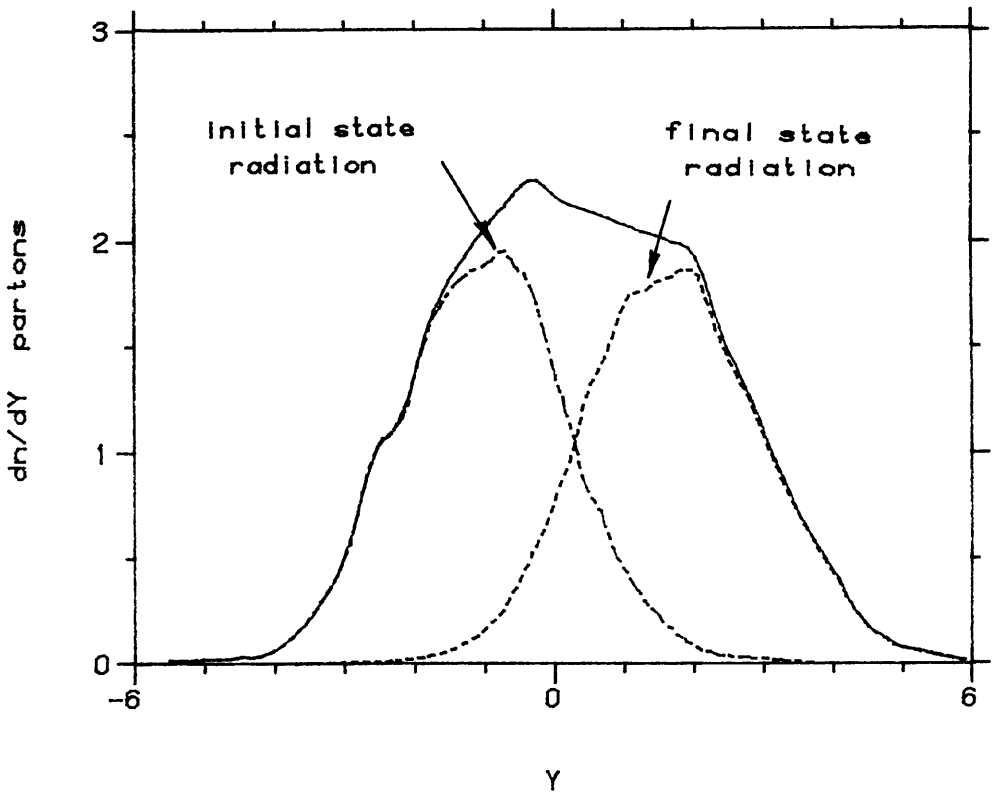
3
2
1
0
dn/dY partons
initial state radiation
final state radiation
-6
0
6
Y

Fig 7 a

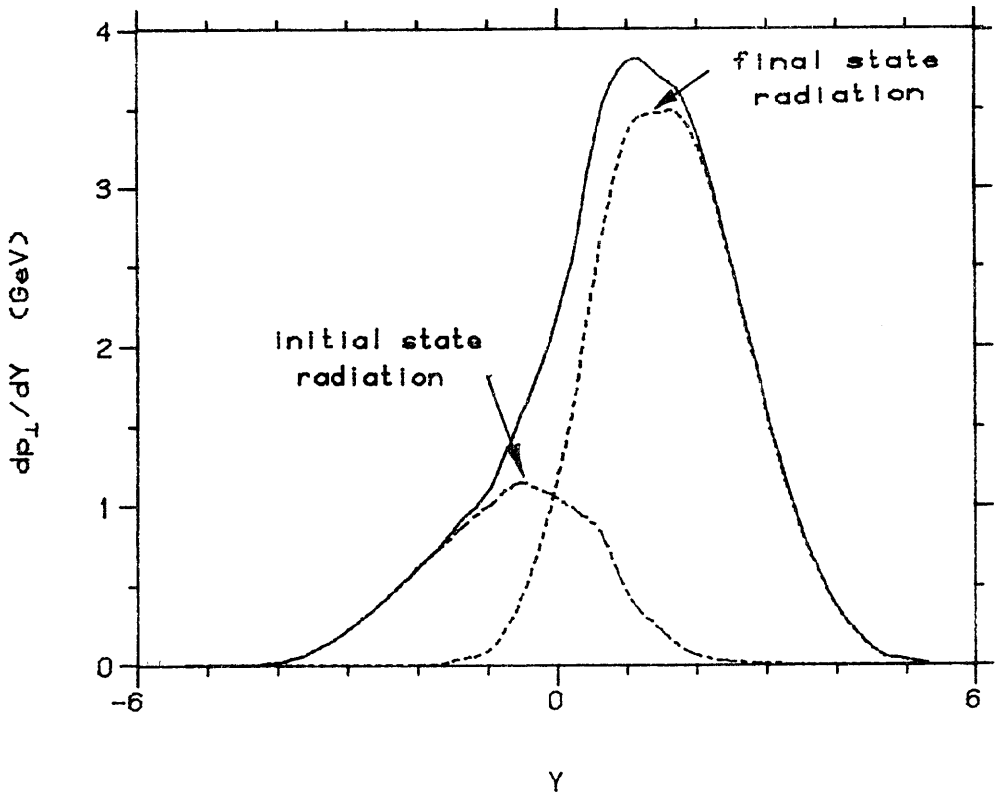
final state
radiation
initial state
radiation
$dp_\perp/dY$ (GeV)
Y
4
3
2
1
0
-6
0
6

Fig 7 b

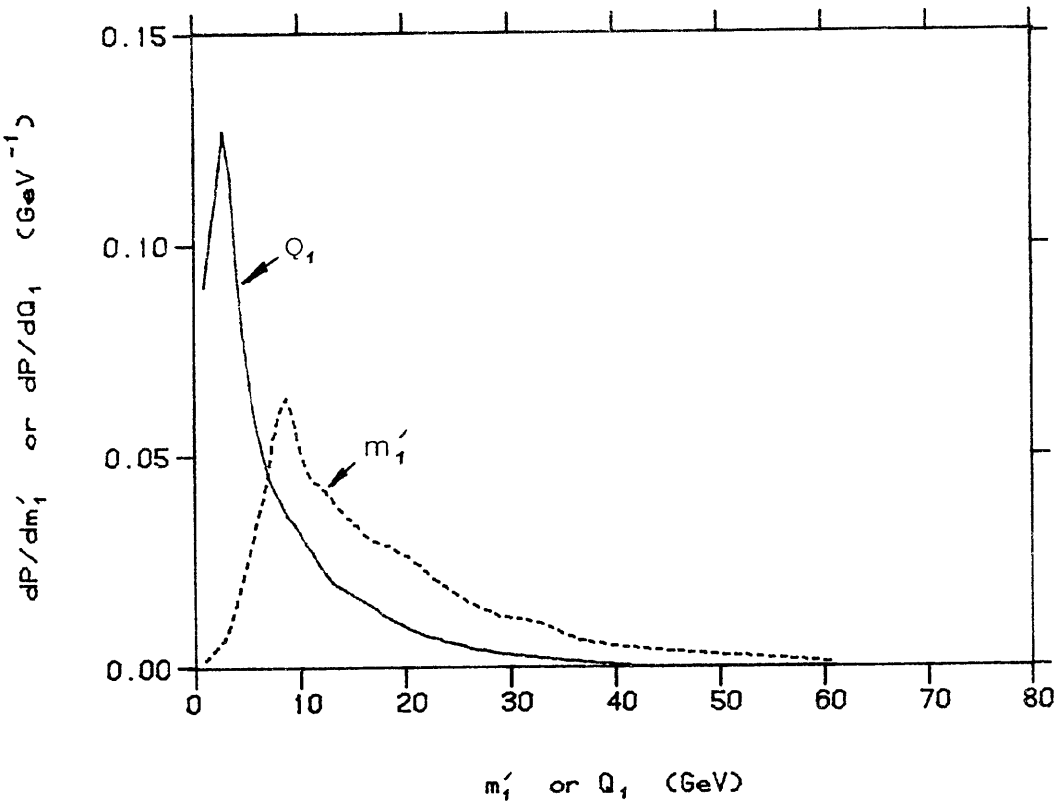
Q_1
m_1'
dP/dm_1' or dP/dQ_1 (GeV^{-1})
m_1' or Q_1 (GeV)
0.15
0.10
0.05
0.00
0
10
20
30
40
50
60
70
80

Fig 8 a

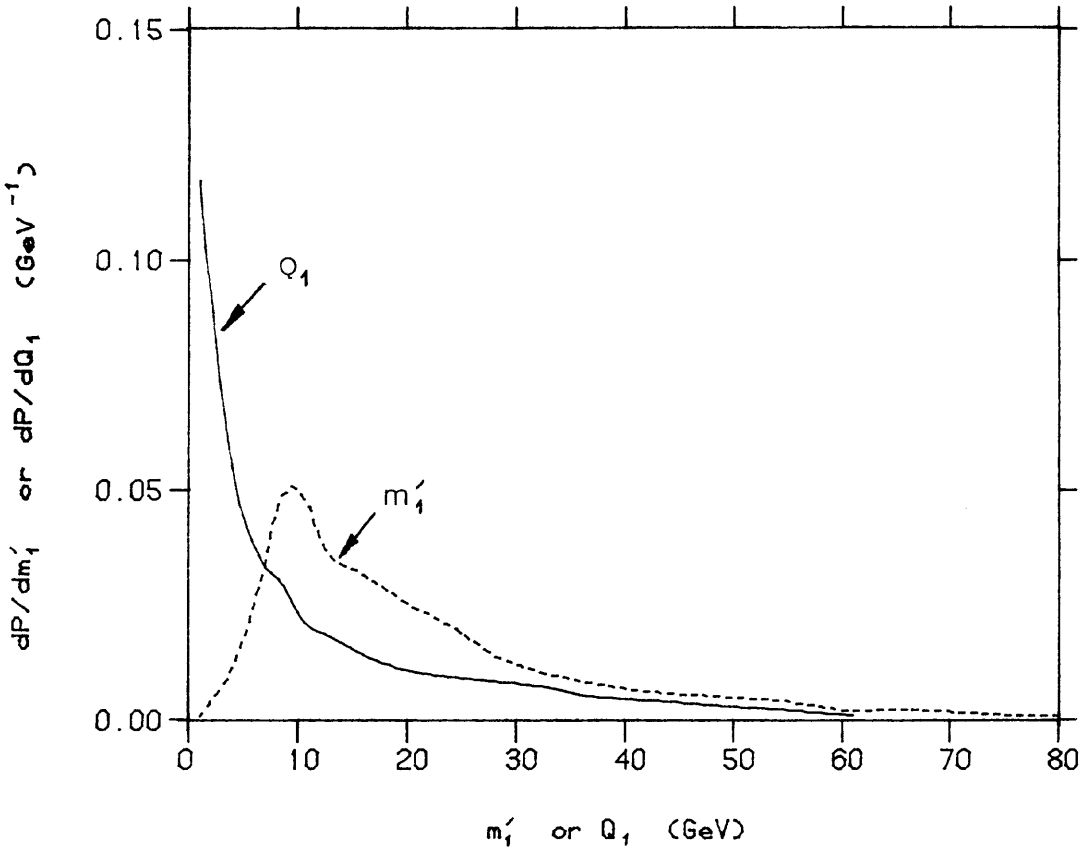
0.15
0.10
0.05
0.00
0
10
20
30
40
50
60
70
80
Q_1
m_1'
dP/dm_1' or dP/dQ_1 (GeV^{-1})
m_1' or Q_1 (GeV)

Fig 8 b

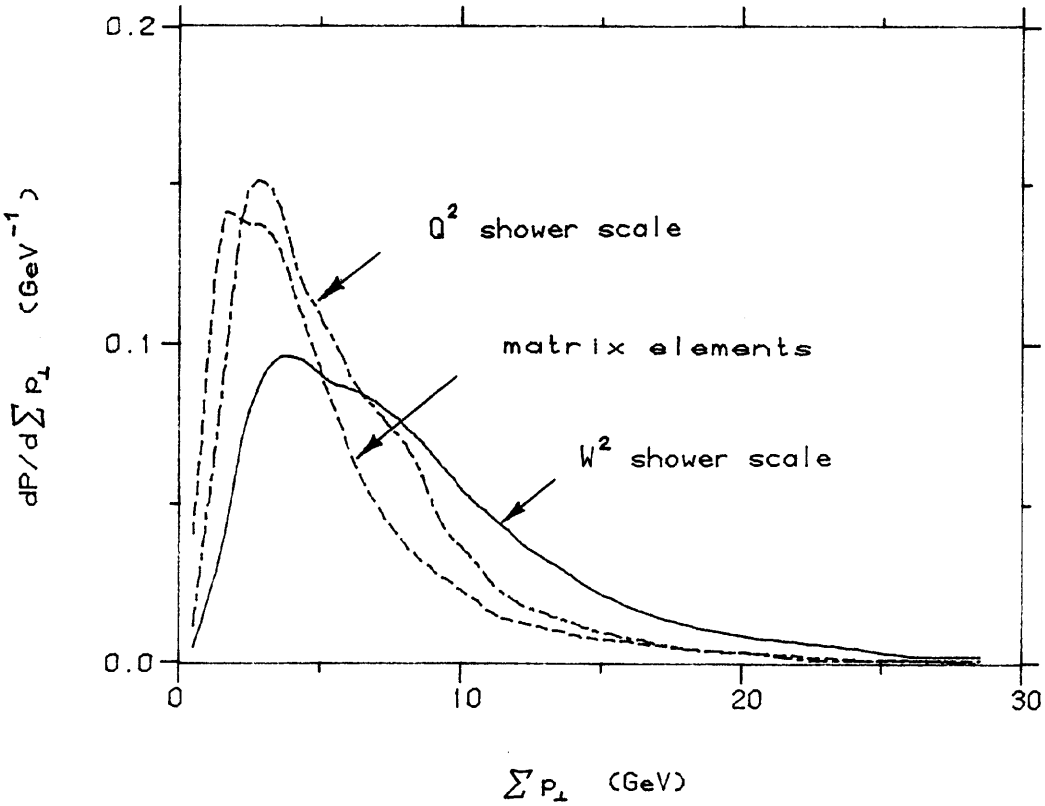
0.2
0.1
0.0
0
10
20
30
Q^2 shower scale
matrix elements
W^2 shower scale
$dP/d\sum p_\perp$ (GeV^{-1})
$\sum p_\perp$ (GeV)

Fig 9

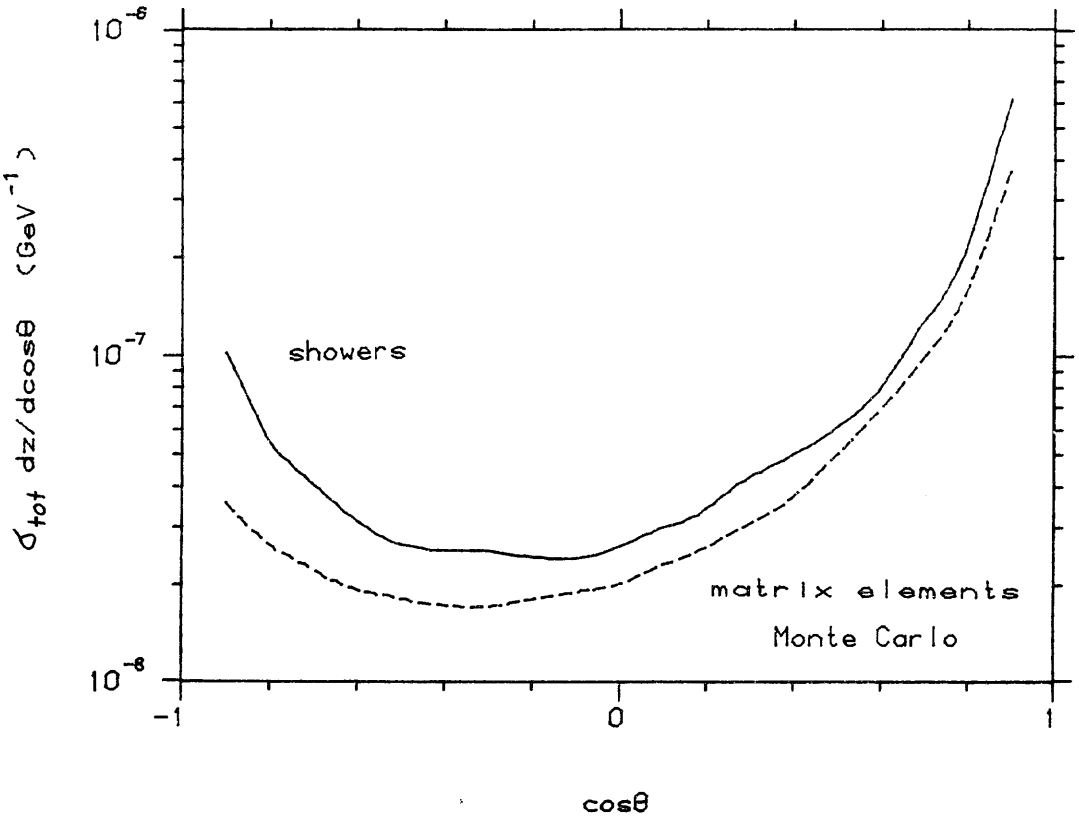

Fig 10

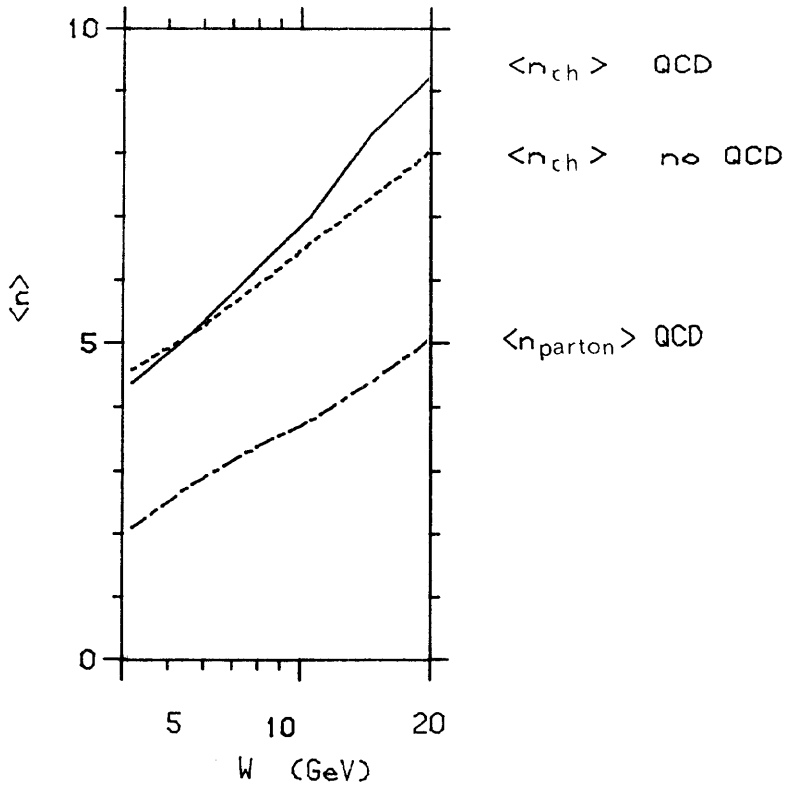

Fig 11a

Fig 12

Fig 11b

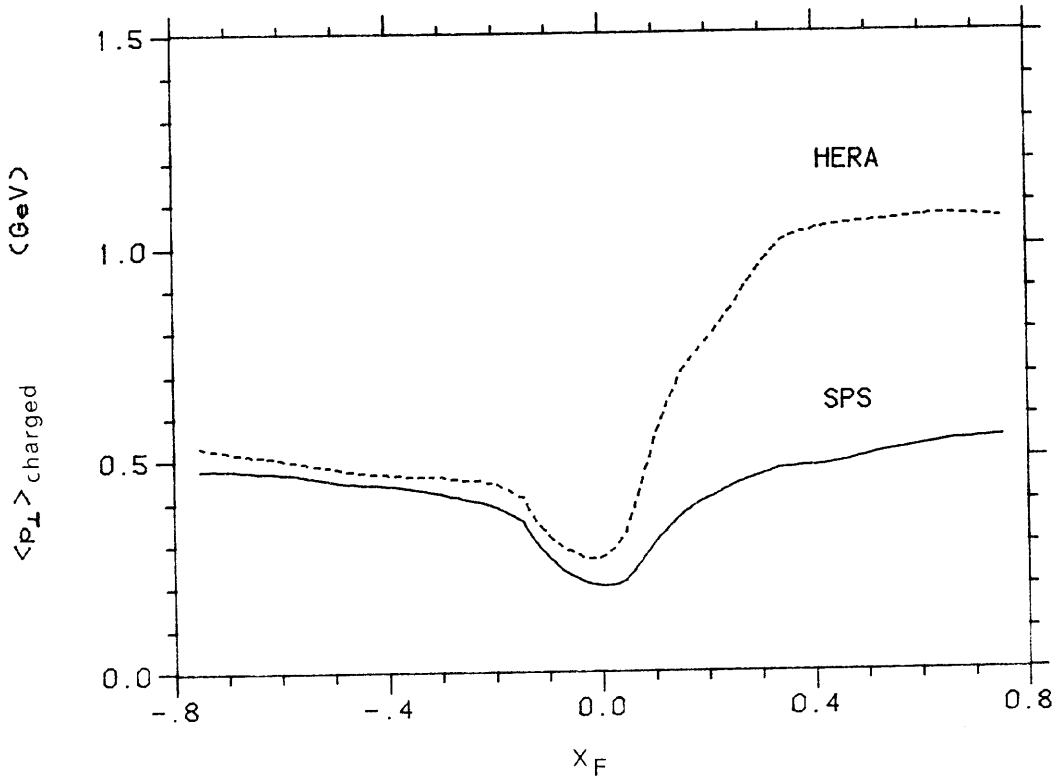

Fig 13